Numerical computations applied to flow and pollutant transport in estuaries

L. Yu,[1] W.N.L. Roma,[1] A.M. Righetto,[1] S. Xo,[2] Z. Geng[2]
[1]*Department of Hydraulics and Sanitary Engineering, School of Engineering at São Carlos, USP, São Carlos, SP, Brazil*
[2]*Zhejiang Institute of Estuarine and Coastal Engineering Research, Hangzhou, China*

Abstract

In this paper, computational examples for analysing the flow and pollutant transport in two estuaries have been briefly presented. In the first example, the impact analysis of seven pollutant sources discharging into a local region of the south estuary of the Yangtze River (China), *19.6km* long and *4.2km* wide, was numerically simulated and predicted over a full tidal cycle by using an unsteady depth-averaged two-dimensional finite volume approach (FVA). In the second example, a nested two- and three-dimensional model was adopted to numerically simulate the complex current patterns in the Hangzhou Bay (China) which is the classical horn-type estuary of the Qiantang River. Depth-averaged two-dimensional finite element modelling was performed in the estuary with an area of about $1400km^2$ and full three-dimensional FVA near-field analyses was applied in the neighbourhood of the intake structure of an electric power plant. These tasks form part of engineering projects in which the authors participated mainly in the numerical computations. Reasonable agreement has been found between the modelled currents and pollutant transport fields, and the experimental as well as observed field data. The results of numerical simulation have been directly used in planning and design of the water cooling systems of the two electric power plants, namely the Shidongkou Second Electric Power Plant (*1.2 million kw*) and the Jiaxing Electric Power Plant (*2.72 million kw*).

1 Introduction

Numerical computation and simulation are powerful tools widely used for planning and engineering design in the coastal water regions. In the past two decades two-dimensional depth-averaged models have been successfully used in simulating and predicting flows and contaminant transport in shallow waters

with different time and length scales to give reasonable results for simulating tidal motions. In the first computational example, the fields of velocity, temperature, COD (*Chemical Oxygen Demand*) and BOD (*Biochemical Oxygen Demand*) concentrations in a local region near the electric power plant were required in order to assess whether the industrial waste-water and waste-heat discharged from the plant would be likely to degrade the regional water environment, where the six waste heat and pollutant sources already existed before the plant was built. The two-dimensional depth-averaged model is utilised to simulate the transport-dispersion of waste heat and contaminants. Our numerical results showed that the discharge of industrial waste water from the new plant had negligible effect on the regional water quality, but the discharge from the existing domestic sewage source, S_4, may have certain influence on the warm waters discharged from the existing electric power plant S_5 and the new one S_7.

In the second computational example, two intakes of the four new turbogenerators of the power plant with the total generating capacity of up to *2.72 million kw* (*4× 0.68 million kw*) are situated about *95m* away from the coast-line of the Yi-Shan, where the sea-bed level generally is in the range *-14.0m* to *-17.5m*. In the outside waters of the Yi-Shan, about *150m~450m* from the bank and *300m* from the axis of the structure to both the west and east sides respectively, the bottom elevation of the pool is from *-20.0m* to *-30.0m*. In addition, there is a deep channel starting from the west end of this deep pool with the bed elevation around *-22.0m* connecting with the outside deep-sea. In order to simulate such a complex flow field, especially to simulate the current movement in the neighbourhood of the power plant, it is necessary to adopt both two- and three-dimensional numerical modelling jointly for analysing the tidal current patterns. As a means of computational fluid mechanics (CFD), finite element method (FEM) and finite different method (FDM) or FVA are two different types of algorithms having their own characteristics and merits. In order to economically provide sufficient numerical information for modelling the flow fields in a large computational domain with complex shape, the authors set up a mixed-dimensional nested model, which does not adopt a unique numerical algorithm, but is composed both of two-dimensional depth-averaged finite element modelling within the whole estuary and nested three-dimensional modelling for the local waters near the structure.

It is significant, and also of great interest either to simulate the pollutant transport and motion caused by the discharge of industrial and domestic effluent into coastline waters or to incorporate one algorithm into another for analysing current patterns in the estuary.

2 Numerical model in the South Estuary of the Yangtze River

The Shidongkou Second Electric Power Plant, with an outlet at S_7 in figure 1, was planned to be built near another existing electric power plant with the outlet S_5 on the south estuary of the Yangtze river. The S_7 outlet was planned to be set up at a location *400m* from the river bank, from which the cooling water

($55.0m^3/s$ and 16^0C) and waste water ($0.39m^3/s$) from an industrial washing process (i.e. water used to wash burnt coal dust) are discharged. In the neighbourhood of the new outlet, there were six other discharging sources (four industrial waste water sources indicated by S_1, S_2, S_3, and S_6, one cooling water source indicated by S_5, also $55.0m^3/s$ and 16^oC, discharging from the existing electric plant, and one sewage source indicated by S_4, $6.94m^3/s$, in figure 1). In order to predict the motion of the warm water bodies and the transport of the pollutant plumes resulting from these discharges, as well as to assess the effect of the main contamination sources on the temperature and water quality of the estuary, a rectangular area S_7 was selected as the computational domain, which is $19.6km$ in length (the x direction) and $4.2km$ in width (the y direction), $7.6km$ from the lower reach and $12km$ to the upper reach of the outlet. A uniform mesh with 100×30 grid points were set up with a resolution of $200m\times 150m$ in the along-river and cross-river directions respectively. The velocity boundary conditions and the variations of local water depth at the entry section of the upper reach were prescribed according to the measured velocities and water elevations of a full tidal cycle in the dry season of 1990. The local tranquil water depth at every grid point was calculated by referring to the topographic map of the estuary in the modelled region.

By considering the variation of bottom topography and water surface, the momentum equations for two-dimensional depth-averaged tidal flows can be written as:[1]

$$\frac{\partial h\bar{u}}{\partial t}+\frac{\partial h\bar{u}^2}{\partial x}+\frac{\partial h\overline{uv}}{\partial y}=-gh\frac{\partial \Delta h}{\partial x}+2\frac{\partial}{\partial x}\left[\frac{\tilde{\nu}_t h}{Re}\frac{\partial \bar{u}}{\partial x}\right]+\frac{\partial}{\partial y}\left[\frac{\tilde{\nu}_t h}{Re}\left(\frac{\partial \bar{u}}{\partial x}+\frac{\partial \bar{v}}{\partial y}\right)\right]$$
$$+\frac{\tau_{sx}}{\rho}-\frac{\tau_{bx}}{\rho}+\bar{S}_{mx}-2\tilde{\nu}_t\frac{\partial u_s}{\partial x}\frac{\partial h}{\partial x}-\tilde{\nu}_t\left(\frac{\partial u_s}{\partial y}+\frac{\partial v_s}{\partial x}\right)\frac{\partial h}{\partial y} \qquad (1)$$

$$\frac{\partial h\bar{v}}{\partial t}+\frac{\partial h\overline{uv}}{\partial x}+\frac{\partial h\bar{v}^2}{\partial y}=-gh\frac{\partial \Delta h}{\partial y}+2\frac{\partial}{\partial y}\left[\frac{\tilde{\nu}_t h}{Re}\frac{\partial \bar{v}}{\partial y}\right]+\frac{\partial}{\partial x}\left[\frac{\tilde{\nu}_t h}{Re}\left(\frac{\partial \bar{u}}{\partial x}+\frac{\partial \bar{v}}{\partial y}\right)\right]$$
$$+\frac{\tau_{sy}}{\rho}-\frac{\tau_{by}}{\rho}+\bar{S}_{my}-\tilde{\nu}_t\left(\frac{\partial v_s}{\partial x}+\frac{\partial u_s}{\partial y}\right)\frac{\partial h}{\partial x}-2\tilde{\nu}_t\frac{\partial v_s}{\partial y}\frac{\partial h}{\partial y} \qquad (2)$$

where '-' stands for depth-averaged values; $\bar{u}$, $\bar{v}$, u_s and v_s represent the depth-averaged velocity components and surface velocities in the x and y directions respectively; $\tilde{\nu}_t$ and Re are depth-averaged turbulent viscosity and Reynolds number; the water-depth $h = z - z_0$ where z and z_0 stand for the elevations of water surface and bottom; Δh is the difference between the h and local tranquil water-depth. The last two additional source terms resulting from the vertical integration involved in the depth-averaged process express the effects of variations of the bottom and surface elevation. Correspondingly, the transport of temperature and concentration of pollutants $\bar{P}$ is governed by:

$$\frac{\partial h\overline{P}}{\partial t}+\frac{\partial h\overline{uP}}{\partial x}+\frac{\partial h\overline{vP}}{\partial y}=\frac{\partial}{\partial x}\left[\frac{h\tilde{\Gamma}_P}{Re}\frac{\partial \overline{P}}{\partial x}\right]+\frac{\partial}{\partial y}\left[\frac{h\tilde{\Gamma}_P}{Re}\frac{\partial \overline{P}}{\partial y}\right]+\overline{S}_P \qquad (3)$$

where $\tilde{\Gamma}_P$ is depth-averaged turbulent eddy diffusion coefficients for temperature or concentration. $\overline{S}_{mx}$, $\overline{S}_{my}$ and $\overline{S}_P$ stand for the source terms resulting from submerged outlets in the momentum and transport equations.

The initial conditions of the velocities, water-depth, temperature and concentration were determined by calculating the steady-state solution of the depth-averaged continuity equations and equations (1)~(3), which can be discretized by use of the FVA associated with water-depth correction coefficients[1]. The time-dependent flow field was computed by pressure-velocity correction algorithm[2]. The source-sink method[3] was used to set up the boundary conditions for the submerged outlets. At the inlet, we set $\overline{u}=U_0(t)$ with $U_0(t)$ being the measured depth-averaged velocity and assumed $\overline{v}=0$. The ambient temperature and concentration were set to 7^oC and 10 *ppm* respectively. At the downstream section, we imposed the zero gradient condition for $\overline{u}$ and $\overline{P}$ and assumed again $\overline{v}=0$. On the open boundary of the selected computational domain, $\overline{u}$ and $\overline{P}$ were all assumed to satisfy approximately the symmetry conditions and $\overline{v}=0$, as this boundary is basically along the centre line of the south branch of the estuary. On the bank, the non-slip boundary conditions were imposed on the tangential velocities, the non-penetrable conditions were imposed for normal velocities and $\overline{P}$ were assumed to satisfy the adiabatic conditions.

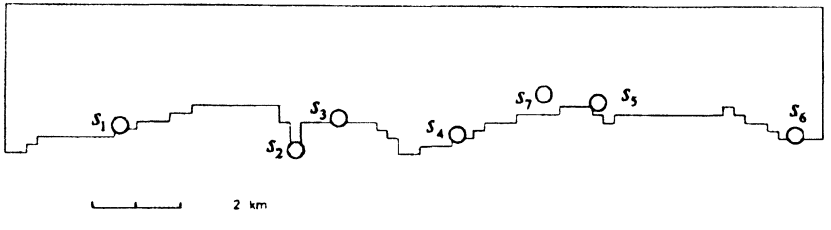


Figure 1: Locations of seven discharge sources

3 Multidimensional nested model for the Hangzhou Bay

In order to simulate well the current patterns in the Hangzhou Bay, the authors first selected a computational domain, which essentially covered all of the estuary with a surface area reaching up to $1400km^2$. Because one of the main purposes of two-dimensional modelling is to offer the time-dependent boundary condition to the succeeding full three-dimensional computation at the near field, it is necessary to concentrate the nodal points in the waters near the intake structure of the Jiaxing Electric Power Plant ($88m^3/s$, see figure 2). The

governing equations adopted the commonly used shallow equations, which involved the Coriolis force and bottom friction and considered the variation of the bottom topography approximately in friction terms. By the use of the Galerkin approach of weighted residual method, the area co-ordinates of the triangular element and the step function as well as lumped mass to result in the shape function, the shallow equations can be discretized with the characteristics based on the explicit scheme for the time-dependent term and upwind scheme for convective terms respectively. A classical tide from the 24th to 26th of May, 1979, was selected as the design tide. The observed variations of the surface elevation and currents at the outside sea could be imposed on the open boundary of the computational domain, the corresponding tidal current on each finite element node could then be solved in terms of the time sequence. The calculations were performed at the time step of *15* seconds, with the non-isotropic eddy viscosity $\varepsilon_x = 30m^2/s$ and $\varepsilon_y = 20m^2/s$.

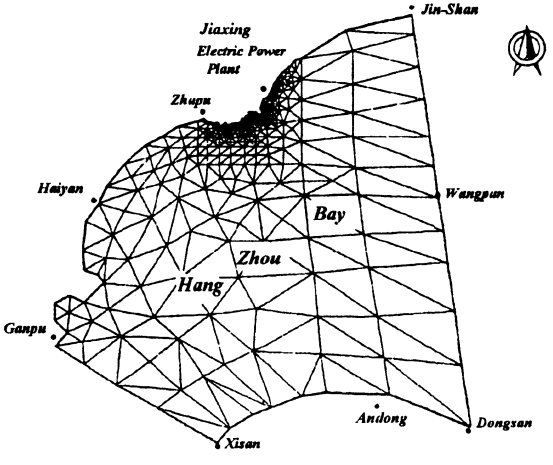


Figure 2: Mesh of two-dimensional finite element computation

Doubtless, merely having the depth-averaged information on a limited number of nodal points is not sufficient for analysing the local current patterns near the intake waters. It is necessary to set up a finer, full three-dimensional model to provide the information in the neighbourhood of the intake structure. In this case, the governing equations in Cartesian co-ordinate are full, non-simplified continuity equation and Reynolds equations for incompressible Newtonian fluid, which are the temporal- or ensemble-averaged forms of the three-dimensional Navier Stokes equations. The three-dimensional governing equations could be discretized in each finite volume into algebraic equations associated with the block technique. By using the FVA and pressure-velocity correction algorithm, a cubic domain $2.15km$ in length, $1.35km$ in width and about $34m$ in depth was selected at the computational domain. A piecewise uniform mesh with $32 \times 24 \times 10$ grid points was set up with a mesh resolution of $100m \times 100m$,

locally densified to $50m \times 50m$ in the central region of horizontal directions, and with an adaptive uniform resolution in the vertical direction respectively. The computational time step in three-dimensional modelling adopted 5~20 *seconds* in terms of the variation of currents, the computational period reaches as far as 26 hours. The SIMPLE-C algorithm was used to couple the unknown variables including the vectorial quantities u, v, w and scalar quantities p. The three open boundaries were made to coincide completely with the corresponding 10 nodal points of two-dimensional modelling, on which the finite element computation had provided the variations of depth-averaged velocity and water elevation every half hour. The piecewise velocity distribution in the vertical direction were used to coincide quantitatively with the velocities on the 10 nodal points of two-dimensional modelling. The water elevation varied each half hour. On the bank and bottom topography, the non-slip and non-penetrable boundary conditions were imposed on the tangential velocities and normal velocities respectively. The initial conditions of velocity and water elevation were determined firstly by calculating the steady-state solution of governing equations and then the time-dependent flow field could be computed.

4 Results and conclusions

The numerical simulation in the south estuary of the Yangtze River provided the necessary information for engineering planning and environmental evaluation; the velocity, temperature, and the concentrations of COD and BOD were output every hour. In all the modelling exercises so far, we ignored the heat exchanged across the water surface, the interaction of wind shear stress applied on the free surface and the regression of waste-heat and pollutants. The variations in COD and BOD due to the reaeration across the surface were also assumed to be negligible, as the computational period is rather short and the computational domain is relatively small. Figure 3 presents the comparison of experimental surface $3^{o}C$ temperature rise region with calculated depth-averaged $3^{o}C$ temperature rise region near the periods of HLW (higher low water) and LHW (lower high water) respectively, where the distance between the S_5 and S_7 was adjusted to $200m$ instead of $1000m$. In figure 3a, the simulated depth-averaged warm water region with $3^{o}C$ temperature rise matches quite well with the data from the experiments. Figure 3b) shows another comparison near the LHW period. The measured surface warm water region in the physical region is generally closed to the area of depth-averaged region with $3^{o}C$ temperature rise computed by the model, but the shape of the warm water region has a rather large difference, which may result from the limitations of physical model experiments. Figure 4 presents the predicted depth-averaged distributions of velocity, temperature, COD and BOD concentrations at the HHW (higher high water) period with the new power plant in operation. Since the effect of water depth has been incorporated in the model with water-depth correction coefficients[1], the computed velocity fields seem to be quite reasonable (see figure 4a): not only the variation of velocity magnitudes but also the variation of velocity directions are influenced by the variation of bottom

topography, especially in the shallow water regions, where the velocities are generally smaller than those in the deep water region. The isotherms of modelled temperature fields are drawn from $7^{o}C$ (background temperature) with $1^{o}C$ interval. The contours of pollutant concentration distributions are drawn from $10ppm$ (background concentration) with a $20\ ppm$ interval. A hot plume is shown to move with the main currents of the river. The temperature with the warm water region increases significantly (e.g. $3.6^{o}C$ at HHW, see figure 4b) and the warm water regions from S_5 and S_7 being all connected, form a big hot plume along the river bank. This is mainly due to the discharge capacity of the waste-heat from both the existing power plant (S_5) and the new plant (S_7), that are quite large, and the cooling water discharged from the submerged outlets that is quickly mixed vertically with the environmental water bodies in the neighbourhood of the outlets, and at the same time diffused and dispersed in the horizontal directions. From our numerical experiments, we also observed that the warm water regions were relatively small during HHW and LLW periods because of strong convection. During periods of slack water, the discharged waste-heat results in larger warm water regions. The strength of the discharged COD is greater than that of BOD, which is well-reflected in the computational results; the number of contours in figure 4d is less than that in figure 4c. The numerical experiments also confirmed the conjecture that S_1, S_2, and S_4 are the main pollutant sources, as there are three peaks in COD concentration in figure 3c near S_1, S_2, and S_4, and two peaks in BOD concentration in figure 4d near S_2 and S_4 respectively. According to the flow rate and concentration of the discharged pollutants at each outlet, S_4 is the main contaminant source with the flowrate up to $Q = 6.96m^3/s$, COD = $300.5ppm$ and BOD = $138.5ppm$. Moreover, due to the fact that outlet S_4 is very close to the outlets of the cooling water S_5 and S_7, the attention should be focused on analysing and evaluating the overlapping region of the pollutant zone and the hot plume. However, because of the strong convection in the estuary of the Yangtze river and highly turbulent flows, the concentrations of COD and BOD near S_5 and S_7 are about of 15 to $30ppm$, but less than $60ppm$ for most of the time. Therefore, although the discharge from S_4 will have some influence, the discharged pollutants from other sources hardly have any influence on the cooling water discharged from the new electric power plant.

Through our model simulation in the south estuary of the Yangtze River, it is found that the discharge of the water used to wash burnt coal dust from the new plant would not significantly change the present water quality of the estuary. It was found, however, that the discharged warm wastes would merge with one another into a large warm water body, which would have a distinct overlapping region with the domestic sewage discharged from S_4. Based on this prediction, it has been suggested that further research on the interaction between the discharge from domestic sewage (S_4) and the discharge from the cooling water (S_5 and S_7) should be performed to determine possible unfavourable impacts.

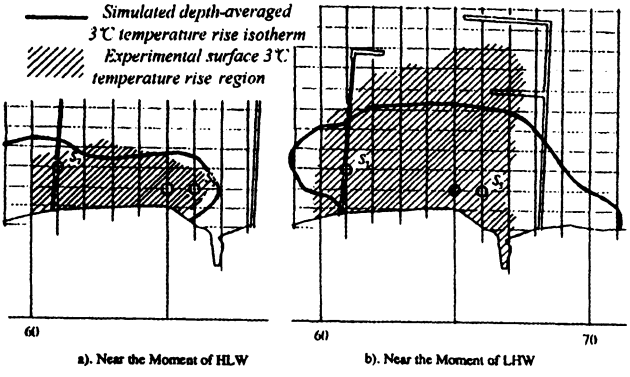


Figure 3: Comparison between surface $3^{o}C$ and depth-averaged $3^{o}C$ rise regions

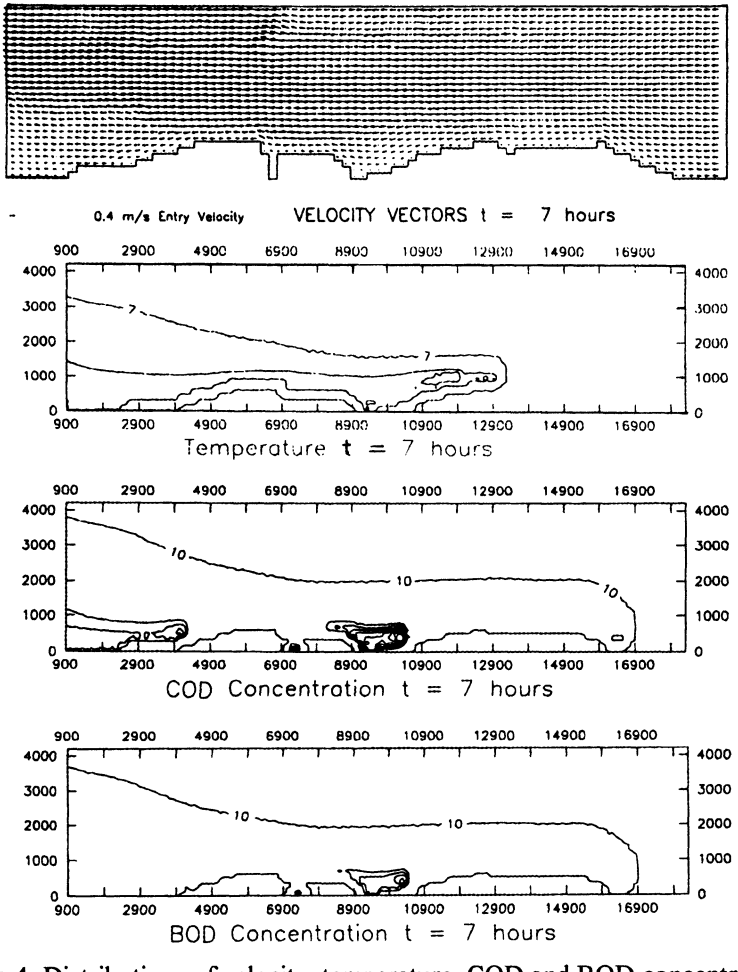


Figure 4: Distributions of velocity, temperature, COD and BOD concentrations

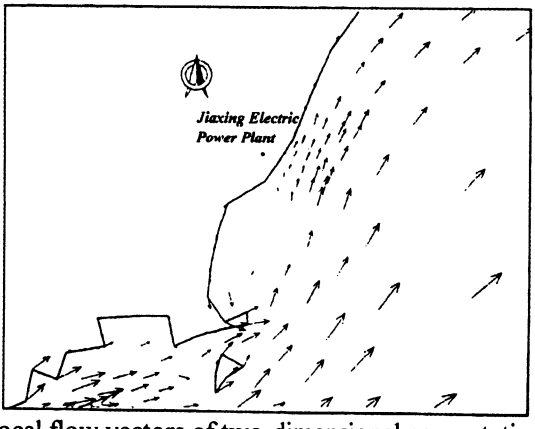


Figure 5: Local flow vectors of two-dimensional computation at the ebb

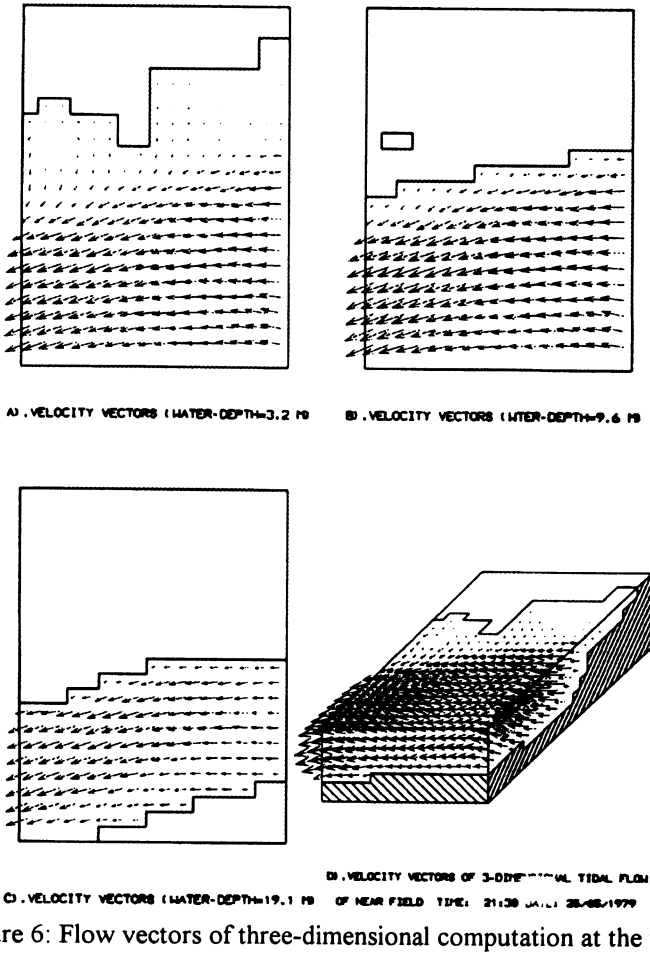


Figure 6: Flow vectors of three-dimensional computation at the flood

Both two-dimensional modelling by using FEM and three-dimensional modelling by FVA for the simulation in the Hangzhou Bay provided abundant numerical results at the discretized nodal points. Figure 5 shows the computed local depth-averaged flow vectors at the ebb. Figure 6 presents computed three-dimensional results on horizontal velocity field including the velocity perspectives during the flood.

The results of three-dimensional modelling have been compared with the field data including both the measured tracks on the water surface and velocity profiles on the vertical near the intake structure. Because the Yi-Shan, at which the intake structure of the plant was constructed, is a hill protruding into the sea, there is an obvious trend to push the current away to a certain extent when the tidal flows change periodically. At the flood, a clear horizontal recirculating flow simulated by three-dimensional modelling exists in the local region of the down reach of the Yi-Shan caused by the association between the stronger currents and jet action. This recirculating flow, however, does not appear in the two-dimensional simulation because of the rather coarse grid and boundary treatment. In addition, the velocity vectors indicate that the tidal currents mainly concentrate in the Yi-Shan deep pool as well as in the corresponding deep channel, where the horizontal velocities become relatively large because of the decrease in water-depth.

Our computations in the Hangzhou Bay have established a nested model. A distinguishing feature of this model is the adoption of two different kinds of numerical algorithms in the mixed-dimensional model for simulating the unsteady tidal currents, which effectively made use of the merits possessed by FEM and FVA respectively. Without doubt, this method can be quite satisfactory for economically and efficiently dealing with the practical problems of fluid motion.

Acknowledgement

The supports of the Processo No. 93/2164-5 of the FAPESP and the Processo No. 301089/94-9(NV) of the CNPq are gratefully acknowledged. Also the authors thank Prof. Fazal H. Chaudhry of the School of Engineering at São Carlos for his useful help on the preparation of this paper.

Reference

1. L. Yu, A new depth-averaged two-dimensional ($\widetilde{k} - \widetilde{w}$) turbulent closure model and its application to numerical simulation for a river, J. of Hydrodynamics **Ser. B**, 1991, **3** (2), 21-28.

2. S.V. Patankar, *Numerical Heat Transfer and Fluid Flow*, Hemisphere Publishing Corporation, 1980.

3. L. Yu, *The turbulent model and numerical research for the turbulent transport of the contaminants in water environment*, Ph.D. Thesis, Hohai University, Nanjing, China, 1988.